OPEN ACCESS Freely available online

PLOS ONE

Dissociation between Brain Amyloid Deposition and Metabolism in Early Mild Cognitive Impairment

Liyong Wu[1,2,3], Jared Rowley[1,2], Sara Mohades[1,2], Antoine Leuzy[1,2], Marina Tedeschi Dauar[1,2], Monica Shin[1,2], Vladimir Fonov[4], Jianping Jia[3], Serge Gauthier[2], Pedro Rosa-Neto[1,2,4]*, the Alzheimer's Disease Neuroimaging Initiative

1 Translational Neuroimaging Laboratory, Douglas Hospital, McGill University, Montreal, Quebec, Canada, **2** McGill Centre for Studies in Aging, McGill University, Montreal, Quebec, Canada, **3** Department of Neurology, Xuan Wu Hospital, Capital Medical University, Beijing, China, **4** McConnell Brain Imaging Centre, Montreal Neurological Institute, McGill University, Montreal, Quebec, Canada

Abstract

Background: The hypothetical model of dynamic biomarkers for Alzheimer's disease (AD) describes high amyloid deposition and hypometabolism at the mild cognitive impairment (MCI) stage. However, it remains unknown whether brain amyloidosis and hypometabolism follow the same trajectories in MCI individuals. We used the concept of early MCI (EMCI) and late MCI (LMCI) as defined by the Alzheimer's disease Neuroimaging Initiative (ADNI)-Go in order to compare the biomarker profile between EMCI and LMCI.

Objectives: To examine the global and voxel-based neocortical amyloid burden and metabolism among individuals who are cognitively normal (CN), as well as those with EMCI, LMCI and mild AD.

Methods: In the present study, 354 participants, including CN (n = 109), EMCI (n = 157), LMCI (n = 39) and AD (n = 49), were enrolled between September 2009 and November 2011 through ADNI-GO and ADNI-2. Brain amyloid load and metabolism were estimated using [^{18}F]AV45 and [^{18}F]fluorodeoxyglucose ([^{18}F]FDG) PET, respectively. Uptake ratio images of [^{18}F]AV45 and [^{18}F]FDG were calculated by dividing the summed PET image by the median counts of the grey matter of the cerebellum and pons, respectively. Group differences of global [^{18}F]AV45 and [^{18}F]FDG were analyzed using ANOVA, while the voxel-based group differences were estimated using statistic parametric mapping (SPM).

Results: EMCI patients showed higher global [^{18}F]AV45 retention compared to CN and lower uptake compared to LMCI. SPM detected higher [^{18}F]AV45 uptake in EMCI compared to CN in the precuneus, posterior cingulate, medial and dorsal lateral prefrontal cortices, bilaterally. EMCI showed lower [^{18}F]AV45 retention than LMCI in the superior temporal, inferior parietal, as well as dorsal lateral prefrontal cortices, bilaterally. Regarding to the global [^{18}F]FDG, EMCI patients showed no significant difference from CN and a higher uptake ratio compared to LMCI. At the voxel level, EMCI showed higher metabolism in precuneus, hippocampus, entorhinal and inferior parietal cortices, as compared to LMCI.

Conclusions: The present results indicate that brain metabolism remains normal despite the presence of significant amyloid accumulation in EMCI. These results suggest a role for anti-amyloid interventions in EMCI aiming to delay or halt the deposition of amyloid and related metabolism impairment.

Citation: Wu L, Rowley J, Mohades S, Leuzy A, Dauar MT, et al. (2012) Dissociation between Brain Amyloid Deposition and Metabolism in Early Mild Cognitive Impairment. PLoS ONE 7(10): e47905. doi:10.1371/journal.pone.0047905

Editor: Stephen D. Ginsberg, Nathan Kline Institute and New York University School of Medicine, United States of America

Received May 25, 2012; **Accepted** September 18, 2012; **Published** October 24, 2012

Funding: The data analysis and writing of this paper were supported by Canadian institutes of Health Research (CIHR) (MOP-11-51-31), Alzheimer's Association (NIRG-08-92090), National Nature Science Foundation of China (NSFC) (3070024), Beijing Scientific and Technological New Star Program (2007B069), Nussia & André Aisenstadt Foundation, and Fonds de la recherche en santé du Québec. Data collection and sharing for this project was funded by the Alzheimer's Disease Neuroimaging Initiative (ADNI) (National Institutes of Health Grant U01 AG024904). The Alzheimer's Disease Neuroimaging Initiative (ADNI) is funded by the National Institute on Aging, the National Institute of Biomedical Imaging and Bioengineering, and through generous contributions from the following: Abbott; Alzheimer's Association; Alzheimer's Drug Discovery Foundation; Amorfix Life Sciences Ltd.; AstraZeneca; Bayer HealthCare; BioClinica, Inc.; Biogen Idec Inc.; Bristol-Myers Squibb Company; Eisai Inc.; Elan Pharmaceuticals Inc.; Eli Lilly and Company; F. Hoffmann-La Roche Ltd and its affiliated company Genentech, Inc.; GE Healthcare; Innogenetics, N.V.; Janssen Alzheimer Immunotherapy Research & Development, LLC.; Johnson & Johnson Pharmaceutical Research & Development LLC.; Medpace, Inc.; Merck & Co., Inc.; Meso Scale Diagnostics, LLC.; Novartis Pharmaceuticals Corporation; Pfizer Inc.; Servier; Synarc Inc.; and Takeda Pharmaceutical Company. The Canadian Institutes of Health Research is providing funds to support ADNI clinical sites in Canada. Private sector contributions are facilitated by the Foundation for the National Institutes of Health (www.fnih.org). The grantee organization is the Northern California Institute for Research and Education, and the study is coordinated by the Alzheimer's Disease Cooperative Study at the University of California, San Diego. ADNI data are disseminated by the Laboratory for Neuro Imaging at the University of California, Los Angeles. This research was also supported by National Institutes of Health grants P30 AG010129 and K01 AG030514. The funders had no role in study design, data collection and analysis, decision to publish, or preparation of the manuscript.

Competing Interests: The Alzheimer's Disease Neuroimaging Initiative study received funding for data collection and sharing from commercial sources (Abbott; Amorfix Life Sciences Ltd.; AstraZeneca; Bayer HealthCare; BioClinica, Inc.; Biogen Idec Inc.; Bristol-Myers Squibb Company; Eisai Inc.; Elan Pharmaceuticals Inc.; Eli Lilly and Company; F. Hoffmann-La Roche Ltd and its affiliated company Genentech, Inc.; GE Healthcare; Innogenetics, N.V.; Janssen Alzheimer Immunotherapy Research & Development, LLC.; Johnson & Johnson Pharmaceutical Research & Development LLC.; Medpace, Inc.; Merck & Co., Inc.; Meso Scale Diagnostics, LLC.; Novartis Pharmaceuticals Corporation; Pfizer Inc.; Servier; Synarc Inc.; and Takeda Pharmaceutical Company.). This does not alter the authors' adherence to all the PLOS ONE policies on sharing data and materials.

* E-mail: pedro.rosa@mcgill.ca

Introduction

Alzheimer's disease (AD) is characterized by a progressive accumulation of amyloid plaques, neurofibrillary tangles and neuronal depletion associated with a slow deterioration of cognition and functional status [1]. Numerous technological advances have made possible the quantification of amyloid accumulation and neurodegeneration in vivo using imaging and fluid biomarkers. In AD, biomarkers are classified as biomarkers of amyloid accumulation (i.e CSF $A\beta_{1-42}$, [^{11}C] Pittsburgh compound B (PIB) Positron Emission Tomography (PET), [^{18}F]AV45 PET) and neurodegeneration (i.e CSF tau, [^{18}F] fluorodeoxyglucose(FDG) PET and structural MRI) [2,3].

Jack [2] proposed a dynamic biomarker model of Alzheimer's based on vivo biomarker observations conducted in elderly normal individuals as well as in mild cognitive impairment (MCI) and AD dementia patients. Jacks' model corroborates the amyloid cascade hypothesis, which posits that the accumulation of β-amyloid acts as an initiating 'upstream' event leading to 'downstream' events such neurodegeneration and subsequent cognitive impairment [2,4]. The dynamic biomarker model of AD describes amyloid accumulation as the dominant biomarker in individuals with predementia, while the combination of amyloid accumulation and neurodegeneration characterize the dementia stage of AD [2]. Moreover, this model predicts a plateau of amyloid accumulation and the onset of brain neurodegeneration as part of the MCI stage of AD [2]. However, the dynamics of amyloid accumulation and neurodegeneration within the MCI stage are not well understood.

Based on the data analysis conducted by the National Alzheimer's Coordinating Center (NACC), the concept of early MCI (EMCI) and late MCI (LMCI) was first introduced by the Alzheimer's Disease Neuroimaging Initiative (ADNI)-Go and ADNI-2 the distinction being made on the basis of modest or advanced impairment of delayed recall of logical memory [5,6]. The concept of EMCI will bridge the gap between normal elderly and LMCI subjects who are more amnestic than EMCI subjects [5]. It should be emphasized that while EMCI subjects still meet criteria for amnestic MCI, they represent a very early point in the clinical spectrum of AD [5,6]. The primary purpose of this classification in ADNI-Go and ADNI-2 is to elucidate the disease mechanisms present at a very early stage of AD (i.e. EMCI), with the attendant objective of improving the efficiency of disease-modification interventions [5,6].

Although several studies have focused on MCI and healthy elderly control, the status of brain amyloid deposition remains unknown at the early stage of MCI. The study from Australian Imaging Biomarkers and Lifestyle Research Group showed that the amyloid load of subjects with subjective cognitive impairment (SCI), a syndrome characterized by subjective memory complaint but no objective memory impairment, was similar to healthy elderly controls, and thus lower than levels found in MCI and AD [7]. Longitudinal studies using [^{11}C]PIB PET have shown no uptake differences during the follow-up of MCI patients who eventually converted to AD, suggesting that amyloid load plateau has been already reached in the late stage of MCI [8,9]. In fact, these findings suggest that LMCI may represent an intermediate state between cognitively normal individuals and MCI.

The existence of synaptic degeneration in EMCI remains to be clarified, particularly due to the presence of mild but objective memory deficits in these individuals. [^{18}F]FDG PET provides qualitative and quantitative estimates of the cerebral metabolic rate of glucose consumption, an index of synaptic functioning and density, which has been proven to be highly related with the clinical symptoms and taken as the symptoms-sensitive measurement in MCI [10,11]. Several studies have shown that MCI patients displayed cerebral hypometabolism bilaterally in the parieto-temporal areas, posterior cingulate cortex (PCC), medial temporal lobe, and even frontal lobe [10,12–14]. It has been suggested that glucose metabolism is a sensitive measure of change in cognition and functional ability in MCI, and has value in predicting future cognitive decline [10,14]. Furthermore, MCI subjects with abnormal glucose metabolism were more likely to convert to AD than subjects who had normal glucose uptake [10–13]. Therefore, [^{18}F]FDG PET provides significant information regarding the clinical characterization of synaptic dysfunction already present in EMCI [3,15].

The main objectives of the present study are thus to examine global and voxel-based neocortical amyloid burden and metabolism within separate groups of cognitively normal (CN), EMCI, LMCI, and AD. We intend to capture the dynamics of amyloid accumulation and neurodegeneration within the MCI stage. Assuming the premises of the amyloid cascade hypothesis, we expect a predominance of amyloid accumulation in the EMCI phase.

Materials and Methods

Database Description

Participants were recruited between September 2009 and November 2011 through ADNI-GO and ADNI-2 from 56 centers in the USA and Canada [16]. The ethics committee at each participating site approved the study protocol. Written consent was obtained from all subjects participating in the study. Inclusion/exclusion criteria for ADNI studies are described elsewhere (https://ida.loni.ucla.edu/login.jsp?project=ADNI).

From the ADNI-Go and ADNI-2 dataset, we selected all participants between 55–90 (inclusive) years of age who had completed, in the same visit, the following clinical, imaging and neuropsychological assessments: MRI, [^{18}F]AV45 PET, [^{18}F]FDG PET, Mini Mental State Examination (MMSE), Clinical Dementia Rating scale (CDR), Wechsler Memory Scale Logical Memory II, Alzheimer's disease assessment scale (ADAS)-cog, Rey auditory verbal learning test (RAVLT), 30-item Boston Naming Test, Category Fluency (animal), and Trails Making Test (A & B), as well as the functional activities questionnaire (FAQ). Selected individuals were classified as CN, LMCI, EMCI and AD according to clinical and behavioral measures provided by ADNI at the time of the imaging study. Individual with Modified Hachinski Ischemia Score higher than four points were excluded during the screening phase. Furthermore, subjects with imaging evidence of clinically significant vascular changes were excluded from this analysis.

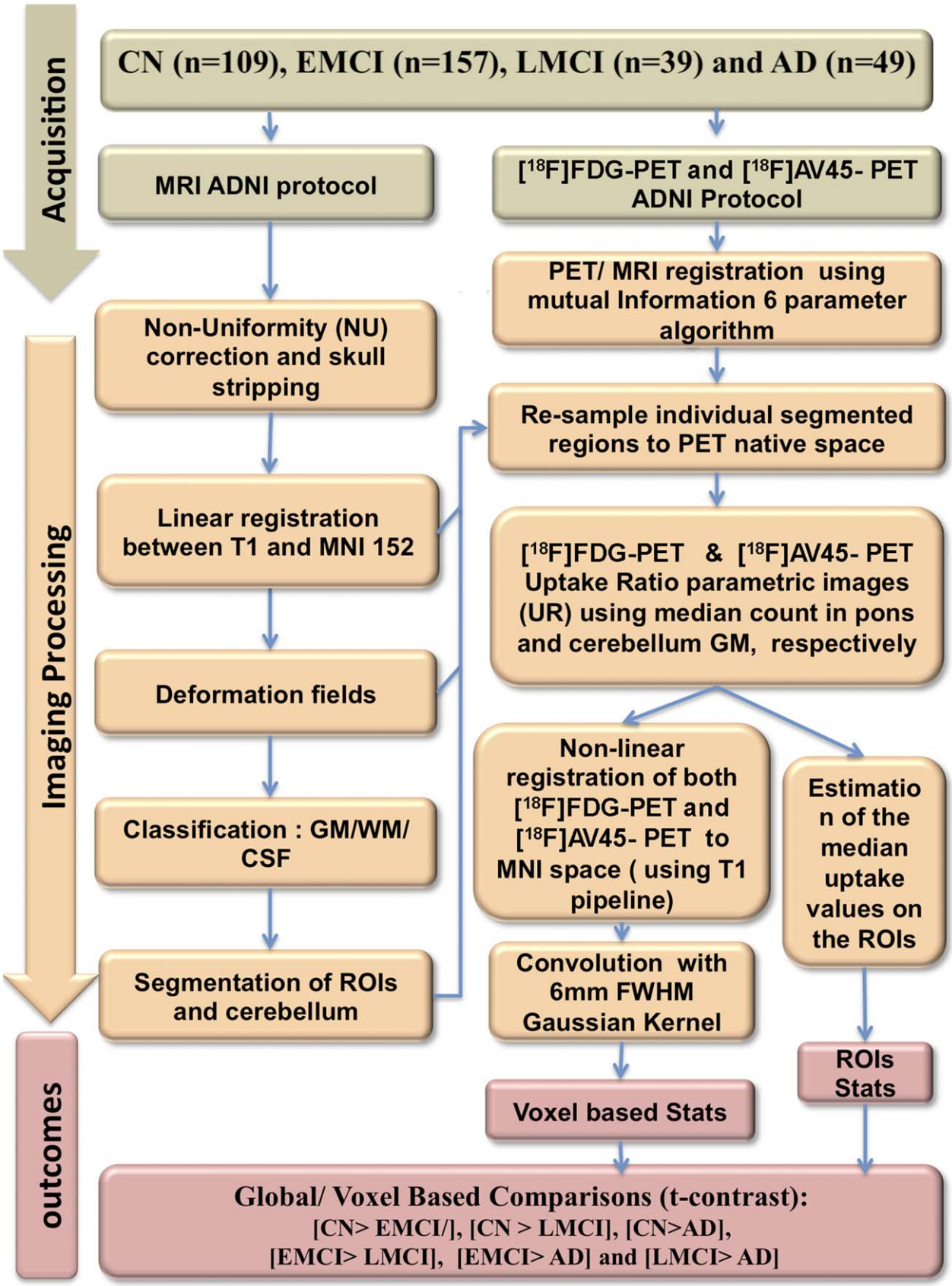

Figure 1. Summary of the imaging analysis methods.
doi:10.1371/journal.pone.0047905.g001

Table 1. Demographics and neuropsychological data for all groups.

	CN (n = 109)	EMCI (n = 157)	LMCI (n = 39)	AD (n = 49)	*p* value
Gender (M/F)	53/56	90/67	24/15	31/18	0.231
Age (years)	78.8±5.9	73.1±7.9[a]	76.2±9.2[d]	75.6±7.8	<0.001
Education (years)	16.4±2.8	16.0±2.7	16.4±3.2	16.7±2.8	0.304
MMSE	29.1±1.2	28.3±1.5[a]	27.1±2.2[a c]	21.4±4.7[a c e]	<0.001
CDR-global	0±0	0.5±0.1[a]	0.5±0.1[a]	1.0±0.4[a c e]	<0.001
CDR-sum of boxes	0.1±0.3	1.3±0.7[a]	1.9±1.4[a c]	5.6±2.5[a c e]	<0.001
ADAS-cog	6.2±4.2	7.9±3.4[a]	12.5±5.7[a c]	21.8±10.3[a c e]	<0.001
Immediate recall of logical memory	14.8±3.6	11.3±3.0[a]	6.5±3.4[a c]	4.2±3.0[a c e]	<0.001
Delayed recall of logical memory	14.0±3.7	9.3±2.1[a]	3.5±2.8[a c]	1.5±2.6[a c e]	<0.001
Total immediate recall of RAVLT (Trial 1 to 5)	45.0±10.6	39.3±11.0[a]	30.0±9.2[a c]	21.1±7.9[a c e]	<0.001
Delayed recall of RAVLT	7.1±4.3	6.1±4.2[b]	2.2±2.8[a c]	0.7±2.3[a c e]	<0.001
Recognition of RAVLT	12.8±2.3	12.2±2.9	9.1±3.8[a c]	6.5±4.3[a c e]	<0.001
Trail making test A	34.6±14.6	36.4±13.1	44.4±24.0[a c]	65.9±38.9[a c e]	<0.001
Trail making test B	82.2±37.1	99.8±57.0[a]	140.1±77.8[a c]	189.6±83.7[a c e]	<0.001
Verbal fluency (animal)	20.8±5.8	18.8±5.0[a]	16.3±5.8[a c]	11.0±4.4[a c e]	<0.001
Boston naming test	27.8±4.4	27.2±3.5	24.9±6.8[a c]	23.2±6.5[a c]	<0.001
FAQ	0.3±1.4	2.3±3.4[a]	5.0±5.4[a c]	15.8±6.5[a c e]	<0.001

All values are indicated as mean ± standard deviation except gender. p value indicates the value for the main effect of each group, as assessed with analyses of variance(ANOVA) for each variable except for gender, where a contingency chi-square was performed. Statistics for post hoc 2-by-2 group comparisons are provided as significant differences:
[a]from CN at $p<0.01$;
[b]from CN at $p<0.05$.
[c]from EMCI at $p<0.01$;
[d]from EMCI at $p<0.05$;
[e]from LMCI at $p<0.01$.
MMSE = mini mental state examination; CDR = clinical dementia rating scale; ADAS = Alzheimer's disease assessment scale; RAVLT = Rey auditory verbal learning test; FAQ = functional activities questionnaire.
doi:10.1371/journal.pone.0047905.t001

Classification Criteria

The criteria for CN included an MMSE score ranging between 24–30 (inclusive), and a CDR score of 0 (non-demented) [17,18]. The criteria for EMCI included the presence of a subjective memory complaint, with an MMSE score between 24–30 (inclusive), objective memory loss as shown on scores on delayed recall of one paragraph from the Wechsler Memory Scale Logical Memory II (adjusted for age and education; ≥16 years: 9–11; 8–15 years: 5–9; 0–7 years: 3–6), a CDR of 0.5, preserved activities of daily living, and an absence of dementia [5,19]. The criteria for LMCI subjects included the same criteria as EMCI, except for the greater objective memory loss measured by scores on delayed recall of Wechsler Memory Scale Logical Memory II (adjusted by age and education; ≥16 years: ≤8; 8–15 years: ≤4; 0–7 years: ≤2) [5]. In addition to the NINCDS/ADRDA criteria for probable AD, mild AD dementia subjects had MMSE scores between 20–26 (inclusive) and a CDR of 0.5 or 1.0 [20].

PET Methods

PET image acquisition. A detailed description of the [^{18}F]AV45 and [^{18}F]FDG PET image acquisition can be found at http://www.adni-info.org and http://www.loni.ucla.edu/ADNI/Data/ADNI_Data.shtml.

PET imaging processing. The image processing is summarized in Figure 1. In brief, T1 MRIs were corrected for non-uniformities and skull stripped. Subsequently, skull-stripped uncorrected MRIs were then linearly registered to the MNI space using mutual information and 9 parameters of transformation. Deformation fields (4 mm) were calculated for each individual scan. Next, the non-linearly registered MRIs were classified into grey matter (GM), white matter (WM) and CSF using the INSECT algorithm. Finally, ANIMAL algorithm extracted the cerebellum, hippocampi as well as the temporal, prefrontal, inferior parietal, anterior and posterior cingulate cortices.

Estimation of parametric images. Individual [^{18}F]AV45 images were registered (see bellow) to the respective structural MRI using a 6 parameter mutual information algorithm. Individual brain regions were subsequently resampled to the PET native space. Uptake ratio (UR) images were calculated by dividing PET image by the median cerebellar grey matter count. Individual UR images were subsequently registered to the MNI space using the respective deformation fields. The images were then blurred using a 6 mm FWHM Gaussian kernel. [^{18}F]FDG UR images were created in the same way as the [^{18}F]AV45 except summed images were obtained using the pons as a reference region.

Estimation of global values. Global cortical [^{18}F]AV45 retention was obtained from the median UR of the prefrontal, orbitofrontal, parietal, temporal, anterior cingulate and posterior cingulate/precuneus for each subject [21]. Global [^{18}F]FDG uptake was formed by the median UR from the inferior parietal cortex, posterior cingulated gyrus, and temporal lobe including the hippocampus.

Table 2. Global [^{18}F]AV45 and [^{18}F]FDG uptake in all groups.

	NC (n = 109)	EMCI (n = 157)	LMCI (n = 39)	AD (n = 49)	*p* value
Global [^{18}F]AV45 retention	1.28±0.25	1.40±0.33[a]	1.56±0.36[a c]	1.62±0.38[a c]	<0.001
Global [^{18}F]FDG uptake	1.40±0.15	1.41±0.16	1.28±0.19[a c]	1.14±0.17[a c e]	<0.001
Regional [^{18}F]FDG uptake					
Left inferior parietal cortex	1.40±0.16	1.42±0.18	1.28±0.21[a c]	1.12±0.18[a c e]	<0.001
Right inferior parietal cortex	1.45±0.17	1.46±0.19	1.33±0.23[a c]	1.16±0.22[a c e]	<0.001
Left temporal lobe	1.35±0.23	1.33±0.16	1.21±0.18[a c]	1.08±0.17[a c e]	<0.001
Right temporal lobe	1.33±0.15	1.38±0.17	1.28±0.18[c]	1.14±0.18[a c e]	<0.001
Left hippocampus	1.18±0.25	1.06±0.12[a]	0.96±0.15[a c]	0.88±0.14[a c]	<0.001
Right hippocampus	1.01±0.11	1.02±0.12	0.92±0.14[a c]	0.84±0.18[a c]	<0.001
Left posterior cingulate cortex	1.58±0.18	1.61±0.20	1.44±0.23[a c]	1.27±0.21[a c e]	<0.001
Right posterior cingulate cortex	1.57±0.19	1.59±0.19	1.42±0.23[a c]	1.25±0.23[a c e]	<0.001

All values are indicated as mean ± standard deviation. p value indicates the value for the main effect of each group, as assessed with analyses of variance(ANOVA) for each variable. Statistics for post hoc 2-by-2 group comparisons are provided as significant differences:
[a]from CN at $p<0.01$;
[b]from CN at $p<0.05$.
[c]from EMCI at $p<0.01$;
[d]from EMCI at $p<0.05$;
[e]from LMCI at $p<0.01$.
doi:10.1371/journal.pone.0047905.t002

Statistical Methods

Statistical tests were performed using SPSS 20.0 statistical software. Statistical significance was set at $p \leq 0.05$.

First, between-group comparisons of demographic and neuropsychological data were assessed using one-way ANOVA or chi-square (for gender) tests accordingly. Pairwise comparisons of CN, EMCI, LMCI and AD subjects were performed using an independence sample t-test.

Secondly, we interrogated [^{18}F]AV45 and [^{18}F]FDG UR at the voxel level in order to localize clusters of significant group difference. Voxel based group statistical differences were obtained by contrasting blurred [^{18}F]FDG and [^{18}F]AV45 UR images from

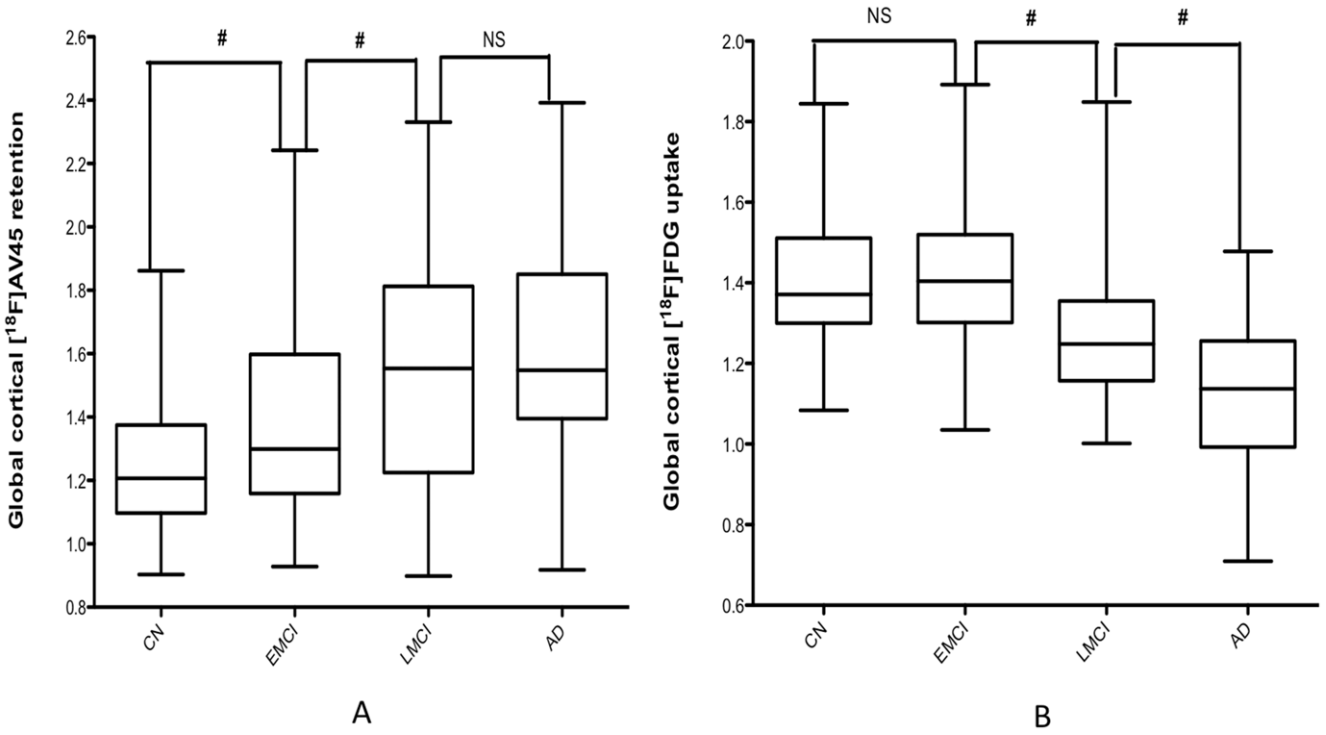

Figure 2. [^{18}F]AV45 (left) and [^{18}F]FDG (right) average images obtained from controls (CN), early MCI (EMCI), late MCI (LMCI) and Alzheimer's dementia patients (AD). In [^{18}F]AV45, there is a reduction of gray and white matter contrast in EMCI, LMCI and AD in comparison with CN. Note the PCC and IPC [^{18}F]FDG SUVR reduction in LMCI and AD in comparison with CN.
doi:10.1371/journal.pone.0047905.g002

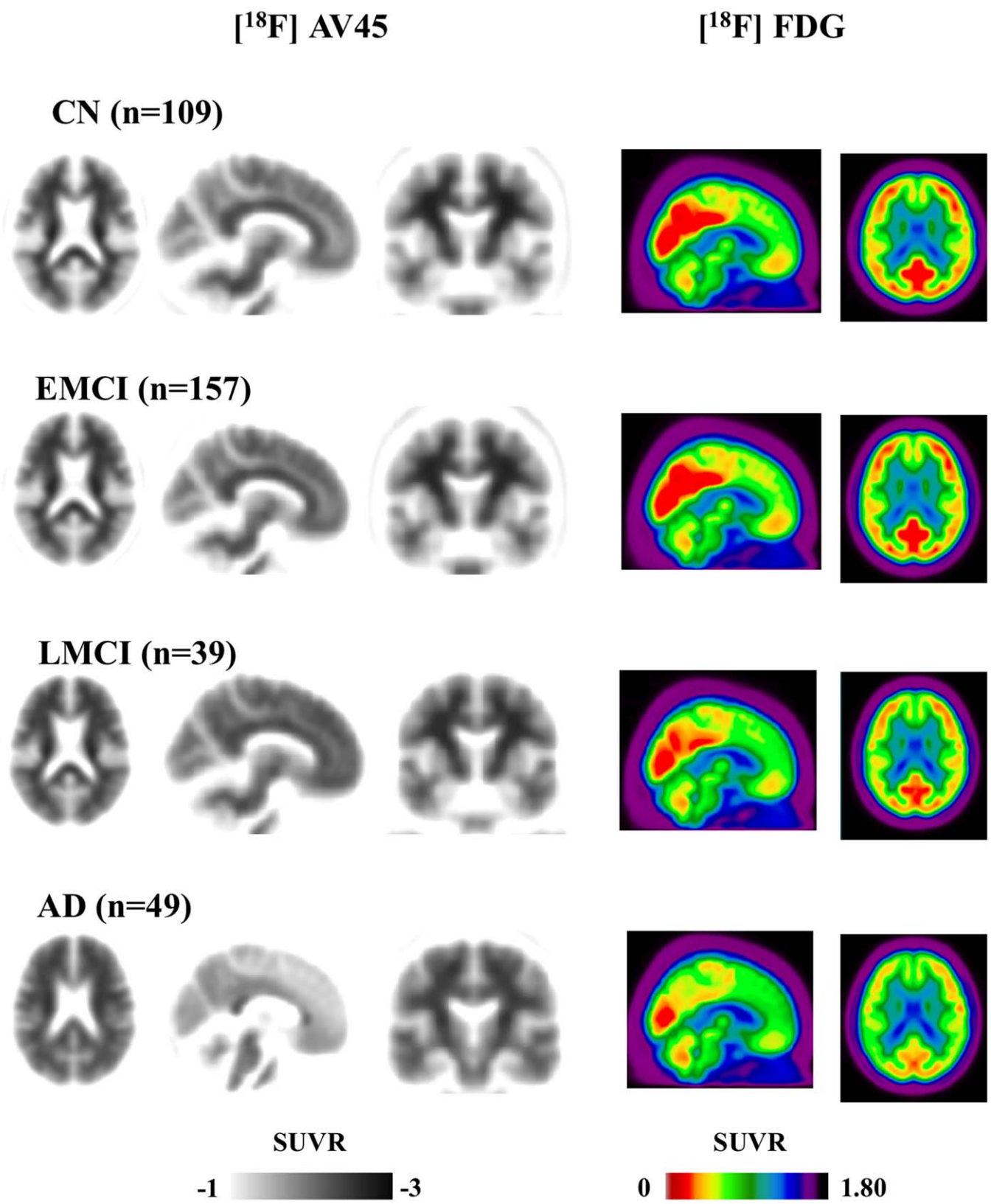

Figure 3. Comparison of global neocortical [^{18}F]AV45 and [^{18}F]FDG uptake among each group. Dissociation of amyloid deposition and hypometabolism in EMCI was shown by significant group difference in term of [^{18}F]AV45 without group difference of [^{18}F]FDG in EMCI versus CN. # means significant difference between groups ($p<0.01$), while NS represents no significant group difference($p>0.05$).
doi:10.1371/journal.pone.0047905.g003

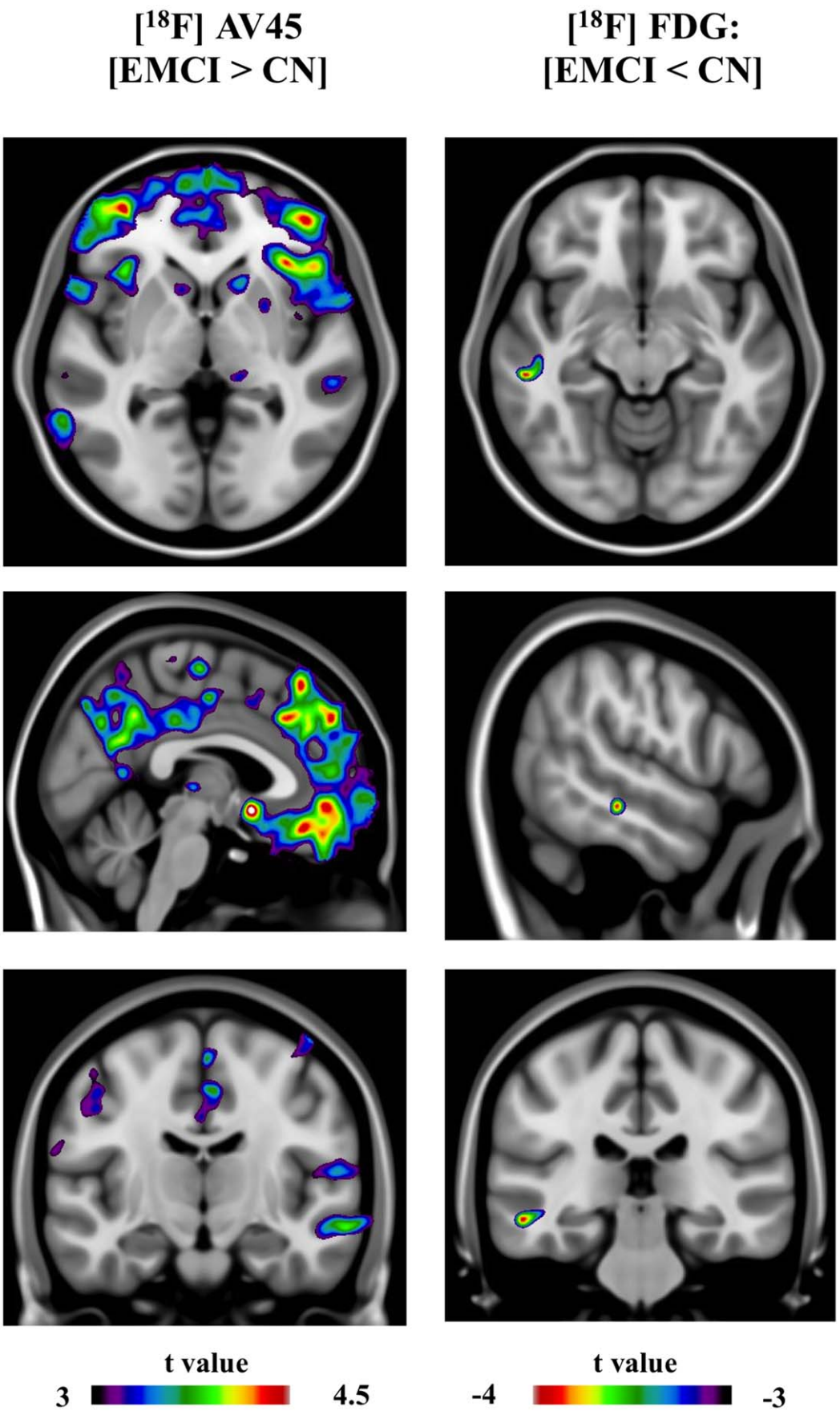
[18F] AV45
[EMCI > CN]
[18F] FDG:
[EMCI < CN]
t value
3
4.5
t value
-4
-3

Figure 4. Images represent statistical parametric mapping depicting (spectrum color bars) t-statistical contrast overlaid on a group structural MRI. Right images represent voxel-based statistical differences comparing [^{18}F]AV45 retention (EMCI > CN). Left images represents voxel-based statistical differences comparing [^{18}F]FDG uptake (EMCI < CN).
doi:10.1371/journal.pone.0047905.g004

all groups, after correcting for age, (2 at a time 6 total contrasts) using RMINC. RMINC is an imaging package that allows images files in the MINC to be analyzed with the powerful statistical environment R-statistic (http://www.r-project.org/). False discovery rate was used to threshold results for multiple comparisons [22]. Corrected threshold of significance was $p<0.01$ a $t>3.5$.

Results

Demographic and Neuropsychological Data

Three hundred fifty-four participants, including CN (n = 109), EMCI (n = 157), LMCI (n = 39) and AD (n = 49), were included in the present study. Demographic data and neuropsychological test scores are shown in Table 1. No significant differences in gender and education were noted among all groups. However, the age of EMCI is younger than CN and LMCI ($p<0.001$, $t = 6.372$, $df = 263$ for EMCI versus CN; $p = 0.032$, $t = 2.159$, $df = 194$ for EMCI versus LMCI).

When the four groups (CN, EMCI, LMCI and AD) were compared, significant differences were found for all neuropsychological scores ($p<0.001$). When compared to CN, EMCI individuals showed significant impairment on the majority of neuropsychological assessment measures, with the exception of trail making test A, recognition of AVLT and Boston naming test. The neuropsychological scores were significantly lower in EMCI patients compared to both LMCI and AD.

Global Cortical [^{18}F]AV45 Retention and [^{18}F]FDG Uptake in Each Group

The global [^{18}F]AV45 retention ratio values in each group are shown in Table 2 and Figure 2. EMCI patients showed significantly higher global [^{18}F]AV45 retention compared to CN (1.40 versus 1.28, $p<0.01$) and lower amyloid retention compared to LMCI (1.40 versus 1.56, $p<0.01$). No significant differences were found between LMCI subjects and AD patients (1.56 versus 1.62, $p = 0.39$). Significance levels remained unchanged after applying age as a covariate.

The global and regional [^{18}F]FDG uptake ratios in each group are shown in Table 2 and Figure 2. No significant differences in global [^{18}F]FDG uptake ratio were found between EMCI subjects and CN individuals (1.42 versus 1.40, $p = 0.233$). In contrast, LMCI patients showed significantly lower global [^{18}F]FDG uptake ratio compared to EMCI (1.28 versus 1.42, $p<0.01$) yet higher than AD (1.28 versus 1.14, $p<0.01$). Significance levels of group difference remained unchanged by the correction of age.

Voxel-based Group Comparisons of [^{18}F]AV45 Retention and [^{18}F]FDG Uptake

[^{18}F]AV45 and [^{18}F]FDG average group images are represented in figure 3. SPM detected significantly higher [^{18}F]AV45 retention in the EMCI subjects compared to CN individuals, mainly in the medial and ventral part of frontal lobe (e.g. medial prefrontal cortex, ventral lateral prefrontal cortex), anterior cingulate cortex (ACC), and posterior cingulate cortex (PCC)/precuneus (figure 4). Compared to EMCI, LMCI subjects showed significantly higher [^{18}F]AV45 retention, most remarkably in dorsal lateral prefrontal cortex (DLPFC), and inferior parietal cortex (IPC), as well as middle temporal cortex (figure 5). Voxel-based analyses revealed a small but significant cluster with higher [^{18}F]AV45 retention in right precentral gyrus in AD patients in contrast to LMCI individuals (figure 6).

SPM analyses revealed a small but significant cluster with lower [^{18}F]FDG uptake in middle temporal gyrus in EMCI patients in contrast to CN (figure 4). Compared to EMCI, LMCI subjects showed significantly lower metabolism, most remarkably in bilateral posterior cingulate cortex (PCC)/precuneus, hippocampus and middle temporal gyrus, and, to a lesser extent, in the inferior parietal cortex (IPC) (figure 5). In contrast to LMCI, AD patients displayed significantly lower [^{18}F]FDG uptake mainly in inferior parietal cortex (IPC) and posterior cingulate cortex (PCC)/precuneus, as well as in the temporal lobe (figure 6).

Discussion

The present study explored, at a global and voxel-based level, brain cortical amyloid burden and metabolism using [^{18}F]AV45 and [^{18}F]FDG, respectively, within separate groups of CN, EMCI, LMCI and AD. We found that the global [^{18}F]AV45 retention level in EMCI is intermediate between that of CN and LMCI, whereas no group differences in global amyloid retention were found between LMCI and AD. As for the global [^{18}F]FDG uptake ratio, EMCI did not show significant differences when compared to CN, while hypometabolism was noticed in LMCI but not in EMCI. In terms of voxel based cortical [^{18}F]AV45 retention, the main finding is that compared to CN, EMCI is associated with a significantly diffuse increased brain amyloid burden. In contrast, only one small hypometabolic cluster was found in the SPM contrast [EMCI < CN], though significant decrements in metabolism were noticed in PCC/precuneus and hippocampus in LMCI versus EMCI.

Amyloid Deposition in EMCI

Abnormal amyloid load is detected in nearly a third of individuals older than 65 y.o. It is relatively well established that abnormal amyloid load is linked to APOE4 status as well as age [23]. A fraction of these individuals might carry, as recently described, reactive amyloidosis [24]. However, the interpretation of these finding remains elusive given the lack of long term longitudinal studies of cognitively normal individuals carriers of high load of amyloid pathology. The amyloid load of subjects with subjective cognitive impairment (SCI) was similar to that found in healthy elderly controls, remaining at a lower level compared with MCI and AD [7]. Longitudinal studies of non-demented older adults have shown that amyloid deposition increases slowly from cognitive normality and precedes cognitive impairment [25,26]. Some of these reports have demonstrated an annual increase of amyloid deposition, in terms of [^{11}C]PIB retention, of 0.9% per year in non-demented older adults, with the amyloid deposition localized to prefrontal, parietal, lateral temporal, and occipital cortices as well as anterior and posterior cingulate cortices [26]. However, it is not known how early in the disease course amyloid deposition can be detected. In the present study, the amyloid burden associated with EMCI is relatively lower than LMCI and higher compared to CN. This finding indicates that amyloid deposition characterizes EMCI stage and will possibly continue to accumulate during the progression from EMCI to LMCI [27].

A 2 year follow-up longitudinal [^{11}C]PIB PET study showed amyloid load in mild AD remained relatively stable, suggesting

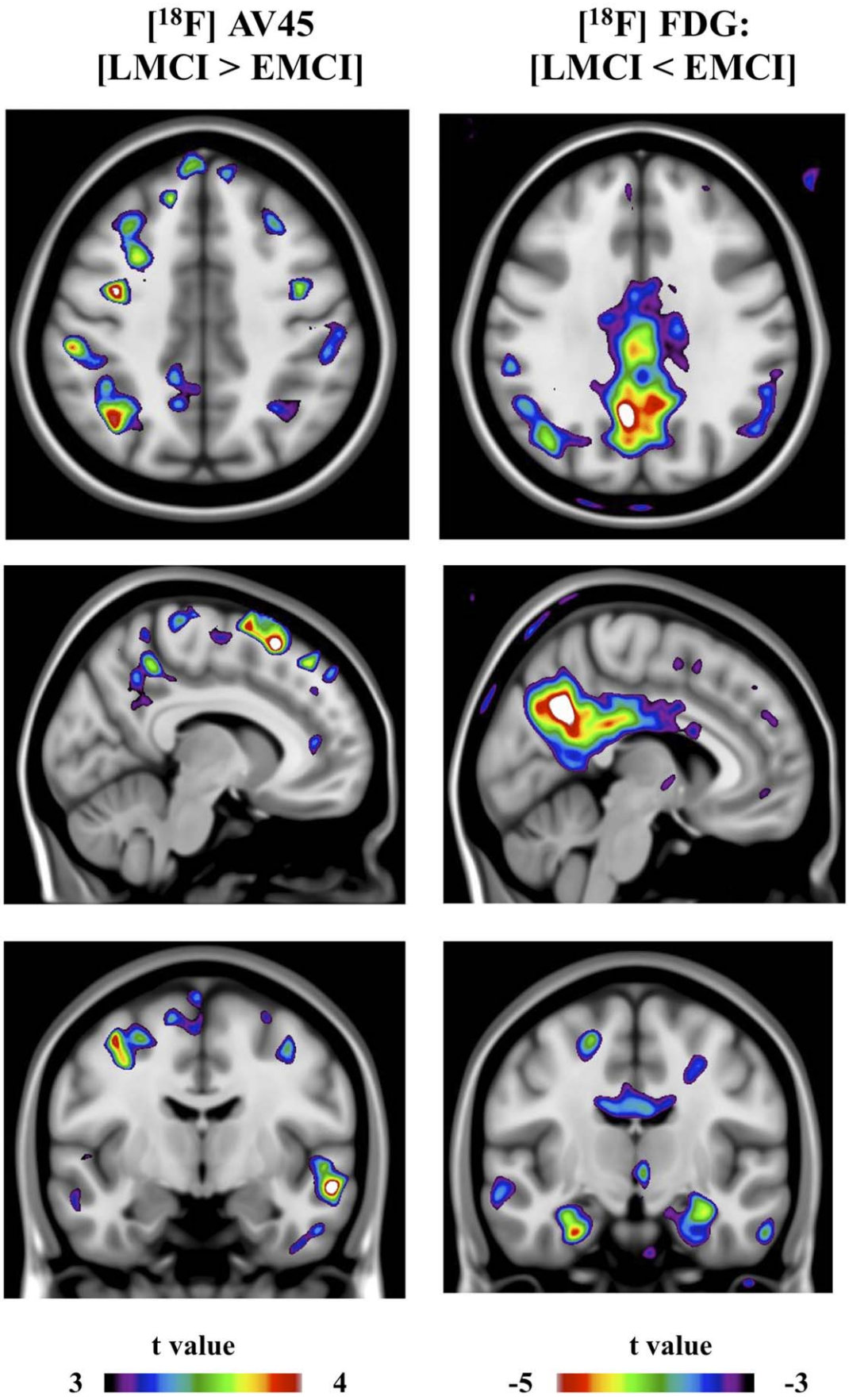

Figure 5. Images represent statistical parametric mapping depicting (spectrum color bars) t-statistical contrast overlaid on a group structural MRI. Right images represent voxel-based statistical differences comparing [^{18}F]AV45 retention (LMCI > EMCI). Left images represents voxel-based statistical differences comparing [^{18}F]FDG uptake (LMCI < EMCI).
doi:10.1371/journal.pone.0047905.g005

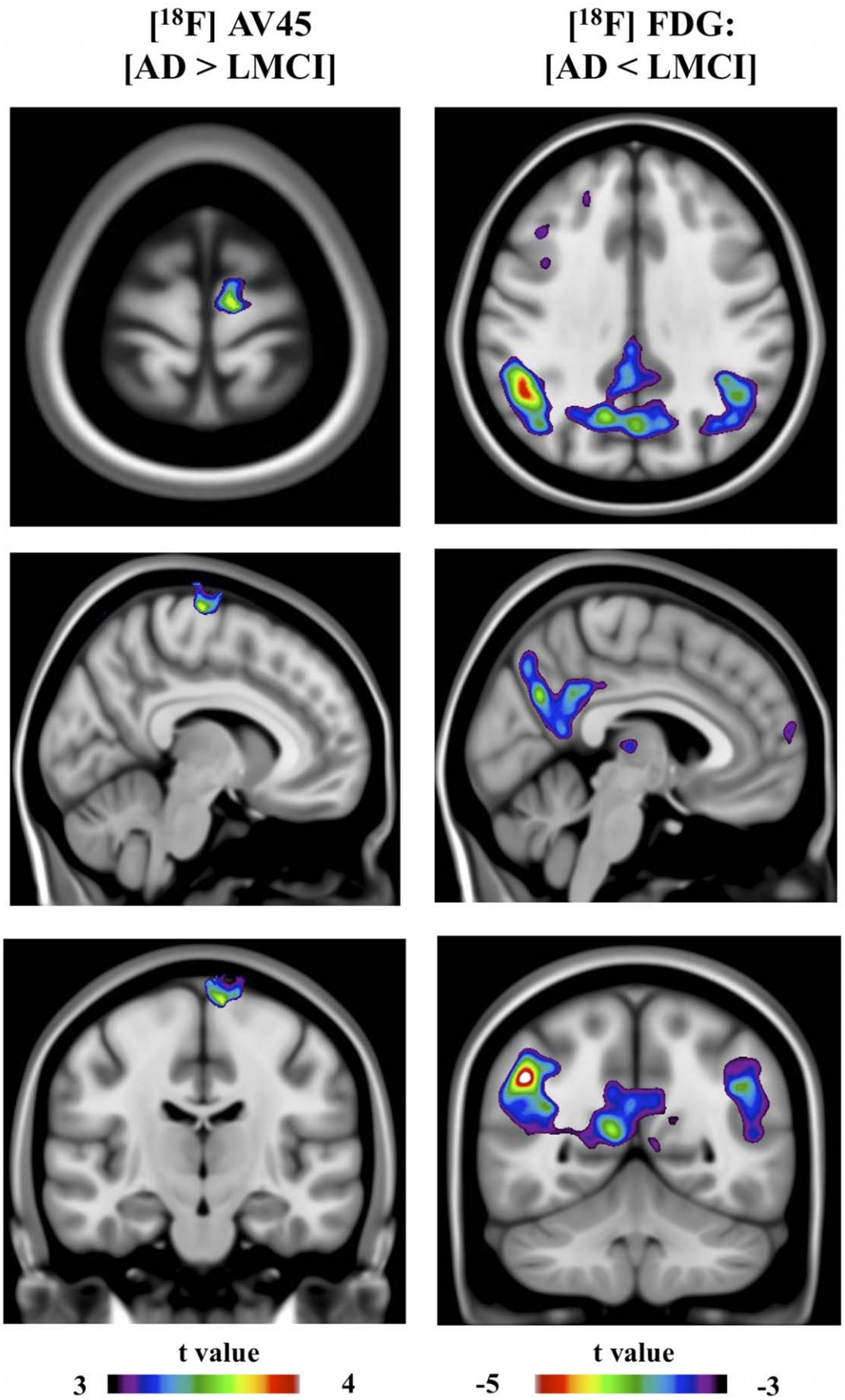
[18F] AV45
[AD > LMCI]
[18F] FDG:
[AD < LMCI]
t value
3
4
t value
-5
-3

Figure 6. Images represent statistical parametric mapping depicting (spectrum color bars) t-statistical contrast overlaid on a group structural MRI. Right images represent voxel-based statistical differences comparing [^{18}F]AV45 retention (AD > LMCI). Left images represents voxel-based statistical differences comparing [^{18}F]FDG uptake (AD < LMCI).
doi:10.1371/journal.pone.0047905.g006

that amyloid deposition in the brain might reach a plateau before the early clinical stages of AD [28]. The concept of amyloid plateau has been further supported by cross sectional studies showing similar amyloid load between MCI and AD, [7,29,30]. Interestingly, other longitudinal studies of MCI cohorts also suggest that the baseline amyloid load could be a predictor of dementia conversion [8,9,21,31]. Together with the previous studies, the absence of group differences in terms of global amyloid retention between LMCI and AD in the present study indicates that amyloid load reaches a plateau at LMCI but not EMCI stage [9,21,29]. Therefore, the findings in the present study further support the dynamic biomarker model of AD, which posits that the amyloid plateau has already been reached in MCI [2].

Interestingly, we found higher amyloid load in ACC/PCC and the inferior part of the frontal lobe in EMCI versus CN, along with higher amyloid burden in temporal and parietal lobe, and superior part of frontal lobe in LMCI versus EMCI. This regional pattern of amyloid deposition is consistent with the pathological process described by autopsy studies where amyloid deposition progress from middle to lateral, from anterior to posterior and from basal to top of the brain [32].

Brain Metabolism in EMCI

The lack of metabolism decrements in EMCI versus CN is possibly associated with a small magnitude in the [^{18}F]FDG metabolism present in early MCI stages as well as the etiological variability within the MCI group. Indeed, variability across studies regarding brain metabolism in MCI occur due to the differences on the diagnostic criteria as well as the variations in clinical severity of the MCI subjects enrolled [12,13,33,34]. Our estimates of global [^{18}F]FDG excluded metabolically stable brain regions in AD in order to increase the sensitivity for detecting hypometabolism. In fact, [^{18}F]FDG-PET studies have shown that medial temporal lobe (MTL), inferior parietal cortex and PCC are vulnerable to hypometabolism and thus appropriated for the identification of MCI, while the utility of other cortical deficits was deemed debatable [34–36]. Moreover, studies focusing on the temporal aspects of progression from MCI to AD conversion have suggested that impairment of [^{18}F]FDG uptake in temporoparietal association cortices predicted a rapid progression to dementia in MCI patients and could, therefore, serve as a biomarker for the diagnosis of prodromal AD [10,15,37].

The most interesting finding of our study is a specific dissociation between brain amyloid deposition and metabolism in EMCI stage. The amyloid load in absence of hypometabolism further supports the view that amyloid deposition precedes neuronal dysfunction in the early stage of MCI [38]. Similarly, the dissociation between amyloid load and metabolic reductions was also demonstrated by another study, in which only 54% of the [^{11}C]PIB positive MCI patients also showed [^{18}F]FDG reductions [34].

Lower [^{18}F]FDG uptake, primarily in bilateral PCC/precuneus and hippocampus, in LMCI versus EMCI supports that brain metabolic dysfunction develop in these regions during the MCI stage and thus might serve as a biomarker to monitor the disease progression from EMCI to LMCI. The present study also raises the question about the role of amyloid plaque formation in the synaptic dysfunction [39]. The group differences between EMCI and LMCI reported in this study support the assumption that brain amyloid deposition is linked with synaptic damage, especially in the PCC/precuneus and hippocampus during the MCI stage, which is of paramount importance vis à vis the use of [^{18}F]FDG PET in clinical trials. Neuronal toxicity might be mediated by high oligomeric forms of $A\beta_{1-42}$ [40–41].

Implications for the Clinical Trial of Disease Modifying Prevention

It is accepted that the use of disease-modifying treatments during the dementia stage of AD may not be adequate, since extensive brain damage has already been established and that the best target population for disease-modifying therapy are those at the MCI stage [3,42]. It is reasonable to assume that the maximal benefit of disease-modifying therapy targeting the amyloid pathophysiologic mechanisms underlying AD should be obtained in the earlier stage before the amyloid load reaches a plateau and irreversible pathological changes occur [3]. The findings in the present study therefore have several important implications. Firstly, the classification of EMCI is a useful concept in terms of early intervention with anti-amyloid therapy. In other words, anti-amyloid therapy should be administered in EMCI instead of LMCI in order to maximize the likelihood of slowing or halt amyloid deposition and thus the downstream pathophysiological processes including the decline of brain metabolism. It is likely that intervention in the late stage of disease would have to target other pathological processes since the amyloid load will have reached a plateau at LMCI stage [7]. Secondly, amyloid imaging can be utilized as a diagnostic biomarker for identifying EMCI individuals, whereas [^{18}F]FDG PET imaging might be used as an endpoint biomarker to monitor the rate of disease progression and detect treatment effects in clinical trials for EMCI [3].

Limitations of the Study

There are several limitations in the interpretation of the present study, which should be acknowledged. Firstly, since the ADNI-GO was initiated 2 years ago and [^{18}F]AV45 and [^{18}F]FDG imaging are to be performed only every two years from baseline, the present data are cross-sectional. Thus, the follow-up of these EMCI patients in ADNI-2 will be of paramount importance to record the real progress of amyloid deposition and metabolism. Secondly, although EMCI patients were carefully selected according to objective memory impairment and exclusion of any significant neurological disease other than suspected incipient AD, EMCI are still likely to encompass heterogeneous etiologies, thereby masking AD-specific findings to some degree. Since no genetic data of new subjects recruited from ADNI-GO and ADNI-2 are currently available for analysis, the impact of Apoe4 on the amyloid deposition is not included in the present study [43]. Finally, despite of the optimal binding to the fibrillary $A\beta_{1-42}$ deposits, [^{18}F]AV45 does not reveal hippocampal $A\beta_{1-42}$ deposits.

Conclusion

The present study explored the global and voxel-based cortical amyloid burden and metabolism within separate groups of CN, EMCI, LMCI, and AD. The present results indicate a dissociation between amyloid deposition and hypometabolism in EMCI. These results highlight the EMCI period as an optimal period for intervention with anti-amyloid therapies.

Author Contributions

Conceived and designed the experiments: LW PR. Performed the experiments: JR LW. Analyzed the data: JR LW PR. Contributed reagents/materials/analysis tools: SM MS VF PR JR. Wrote the paper: LW SM AL MD MS JJ SG PR.

References

1. Ballard C, Gauthier S, Corbett A, Brayne C, Aarsland D, et al. (2011) Alzheimer's disease. Lancet 377: 1019–1031.
2. Jack CR Jr, Knopman DS, Jagust WJ, Shaw LM, Aisen PS, et al. (2010) Hypothetical model of dynamic biomarkers of the Alzheimer's pathological cascade. Lancet Neurol 9: 119–128.
3. Wu L, Rosa-Neto P, Gauthier S (2011) Use of biomarkers in clinical trials of Alzheimer disease: from concept to application. Mol Diagn Ther 15: 313–325.
4. Hardy JA, Higgins GA (1992) Alzheimer's disease: the amyloid cascade hypothesis. Science 256: 184–185.
5. Aisen PS, Petersen RC, Donohue MC, Gamst A, Raman R, et al. (2010) Clinical Core of the Alzheimer's Disease Neuroimaging Initiative: progress and plans. Alzheimers Dement 6: 239–246.
6. Weiner MW, Aisen PS, Jack CR Jr, Jagust WJ, Trojanowski JQ, et al. (2010) The Alzheimer's disease neuroimaging initiative: progress report and future plans. Alzheimers Dement 6: 202–211 e207.
7. Chetelat G, Villemagne VL, Bourgeat P, Pike KE, Jones G, et al. (2010) Relationship between atrophy and beta-amyloid deposition in Alzheimer disease. Ann Neurol 67: 317–324.
8. Okello A, Koivunen J, Edison P, Archer HA, Turkheimer FE, et al. (2009) Conversion of amyloid positive and negative MCI to AD over 3 years: an 11C-PIB PET study. Neurology 73: 754–760.
9. Koivunen J, Scheinin N, Virta JR, Aalto S, Vahlberg T, et al. (2011) Amyloid PET imaging in patients with mild cognitive impairment: a 2-year follow-up study. Neurology 76: 1085–1090.
10. Landau SM, Harvey D, Madison CM, Koeppe RA, Reiman EM, et al. (2010) Associations between cognitive, functional, and FDG-PET measures of decline in AD and MCI. Neurobiol Aging 32: 1207–1218.
11. Mosconi L, Berti V, Glodzik L, Pupi A, De Santi S, et al. (2010) Pre-clinical detection of Alzheimer's disease using FDG-PET, with or without amyloid imaging. J Alzheimers Dis 20: 843–854.
12. Langbaum JB, Chen K, Lee W, Reschke C, Bandy D, et al. (2009) Categorical and correlational analyses of baseline fluorodeoxyglucose positron emission tomography images from the Alzheimer's Disease Neuroimaging Initiative (ADNI). Neuroimage 45: 1107–1116.
13. Mosconi L, Tsui WH, De Santi S, Li J, Rusinek H, et al. (2005) Reduced hippocampal metabolism in MCI and AD: automated FDG-PET image analysis. Neurology 64: 1860–1867.
14. Chen K, Langbaum JB, Fleisher AS, Ayutyanont N, Reschke C, et al. (2010) Twelve-month metabolic declines in probable Alzheimer's disease and amnestic mild cognitive impairment assessed using an empirically pre-defined statistical region-of-interest: findings from the Alzheimer's Disease Neuroimaging Initiative. Neuroimage 51: 654–664.
15. Landau SM, Harvey D, Madison CM, Reiman EM, Foster NL, et al. (2010) Comparing predictors of conversion and decline in mild cognitive impairment. Neurology 75: 230–238.
16. Weiner MW, Veitch DP, Aisen PS, Beckett LA, Cairns NJ, et al. (2011) The Alzheimer's Disease Neuroimaging Initiative: A review of papers published since its inception. Alzheimers Dement.
17. Berg L (1988) Clinical Dementia Rating (CDR). Psychopharmacol Bull 24: 637–639.
18. Folstein MF, Folstein SE, McHugh PR (1975) "Mini-mental state". A practical method for grading the cognitive state of patients for the clinician. J Psychiatr Res 12: 189–198.
19. Wechsler D (1987) WMS-R Wechsler Memory Scale-Revised Manual. New York: The Psychological Corporation, Harcourt Brace Javanovick, Inc.
20. Tierney MC, Fisher RH, Lewis AJ, Zorzitto ML, Snow WG, et al. (1988) The NINCDS-ADRDA Work Group criteria for the clinical diagnosis of probable Alzheimer's disease: a clinicopathologic study of 57 cases. Neurology 38: 359–364.
21. Jack CR Jr, Wiste HJ, Vemuri P, Weigand SD, Senjem ML, et al. (2010) Brain beta-amyloid measures and magnetic resonance imaging atrophy both predict time-to-progression from mild cognitive impairment to Alzheimer's disease. Brain 133: 3336–3348.
22. Worsley KJ, Taylor JE, Tomaiuolo F, Lerch J (2004) Unified univariate and multivariate random field theory. Neuroimage 23 Suppl 1: S189–195.
23. Morris J (2010) CDR ACTUAL PROTOCOL. 1–10.
24. Soscia SJ, Kirby JE, Washicosky KJ, Tucker SM, Ingelsson M, et al. (2010) The Alzheimer's Disease-Associated Amyloid β-Protein Is an Antimicrobial Peptide. PLoS ONE 5: e9505.
25. Villemagne VL, Pike KE, Chetelat G, Ellis KA, Mulligan RS, et al. (2011) Longitudinal assessment of Abeta and cognition in aging and Alzheimer disease. Ann Neurol 69: 181–192.
26. Sojkova J, Zhou Y, An Y, Kraut MA, Ferrucci L, et al. (2011) Longitudinal patterns of beta-amyloid deposition in nondemented older adults. Arch Neurol 68: 644–649.
27. Aizenstein HJ, Nebes RD, Saxton JA, Price JC, Mathis CA, et al. (2008) Frequent amyloid deposition without significant cognitive impairment among the elderly. Arch Neurol 65: 1509–1517.
28. Engler H, Forsberg A, Almkvist O, Blomquist G, Larsson E, et al. (2006) Two-year follow-up of amyloid deposition in patients with Alzheimer's disease. Brain 129: 2856–2866.
29. Jack CR Jr, Lowe VJ, Weigand SD, Wiste HJ, Senjem ML, et al. (2009) Serial PIB and MRI in normal, mild cognitive impairment and Alzheimer's disease: implications for sequence of pathological events in Alzheimer's disease. Brain 132: 1355–1365.
30. Weigand SD, Vemuri P, Wiste HJ, Senjem ML, Pankratz VS, et al. (2011) Transforming cerebrospinal fluid Abeta42 measures into calculated Pittsburgh Compound B units of brain Abeta amyloid. Alzheimers Dement 7: 133–141.
31. Forsberg A, Engler H, Almkvist O, Blomquist G, Hagman G, et al. (2008) PET imaging of amyloid deposition in patients with mild cognitive impairment. Neurobiol Aging 29: 1456–1465.
32. Braak H, Braak E (1991) Neuropathological stageing of Alzheimer-related changes. Acta Neuropathol 82: 239–259.
33. Del Sole A, Clerici F, Chiti A, Lecchi M, Mariani C, et al. (2008) Individual cerebral metabolic deficits in Alzheimer's disease and amnestic mild cognitive impairment: an FDG PET study. Eur J Nucl Med Mol Imaging 35: 1357–1366.
34. Li Y, Rinne JO, Mosconi L, Pirraglia E, Rusinek H, et al. (2008) Regional analysis of FDG and PIB-PET images in normal aging, mild cognitive impairment, and Alzheimer's disease. Eur J Nucl Med Mol Imaging 35: 2169–2181.
35. Devanand DP, Mikhno A, Pelton GH, Cuasay K, Pradhaban G, et al. (2010) Pittsburgh compound B (11C-PIB) and fluorodeoxyglucose (18 F-FDG) PET in patients with Alzheimer disease, mild cognitive impairment, and healthy controls. J Geriatr Psychiatry Neurol 23: 185–198.
36. Mosconi L (2005) Brain glucose metabolism in the early and specific diagnosis of Alzheimer's disease. FDG-PET studies in MCI and AD. Eur J Nucl Med Mol Imaging 32: 486–510.
37. Herholz K (2010) Cerebral glucose metabolism in preclinical and prodromal Alzheimer's disease. Expert Rev Neurother 10: 1667–1673.
38. Lowe VJ, Kemp BJ, Jack CR Jr, Senjem M, Weigand S, et al. (2009) Comparison of 18F-FDG and PiB PET in cognitive impairment. J Nucl Med 50: 878–886.
39. Edison P, Archer HA, Hinz R, Hammers A, Pavese N, et al. (2007) Amyloid, hypometabolism, and cognition in Alzheimer disease: an [11C]PIB and [18F]FDG PET study. Neurology 68: 501–508.
40. Renner M, Lacor PN, Velasco PT, Xu J, Contractor A, et al. (2010) Deleterious Effects of Amyloid β Oligomers Acting as an Extracellular Scaffold for mGluR5. Neuron 66: 739–754.
41. Lacor PN, Buniel MC, Furlow PW, Sanz Clemente A, Velasco PT, et al. (2007) A Oligomer-Induced Aberrations in Synapse Composition, Shape, and Density Provide a Molecular Basis for Loss of Connectivity in Alzheimer's Disease. The Journal of neuroscience : the official journal of the Society for Neuroscience 27: 796–807.
42. Cummings JL, Doody R, Clark C (2007) Disease-modifying therapies for Alzheimer disease: challenges to early intervention. Neurology 69: 1622–1634.
43. Reiman EM, Chen K, Liu X, Bandy D, Yu M, et al. (2009) Fibrillar amyloid-beta burden in cognitively normal people at 3 levels of genetic risk for Alzheimer's disease. Proc Natl Acad Sci U S A 106: 6820–6825.